

Twin-Load: Building a Scalable Memory System over the Non-Scalable Interface

Zehan Cui^{1,2} Tianyue Lu^{1,2} Haiyang Pan^{1,2} Sally A. Mckee³ Mingyu Chen^{1*}

¹Institute of Computing Technology, Chinese Academy of Sciences, Beijing, China

²University of Chinese Academy of Sciences, Beijing, China

³Chalmers University of Technology, Sweden

{cuizehan, lutianyue, panhaiyang}@ict.ac.cn mckee@chalmers.se cmy@ict.ac.cn

Abstract

Commodity memory interfaces have difficulty in scaling memory capacity to meet the needs of modern multicore and big data systems. DRAM device density and maximum device count are constrained by technology, package, and signal integrity issues that limit total memory capacity. Synchronous DRAM protocols require data to be returned within a fixed latency, and thus memory extension methods over commodity DDRx interfaces fail to support scalable topologies. Current extension approaches either use slow PCIe interfaces, or require expensive changes to the memory interface, which limits commercial adoptability.

*Here we propose **twin-load**, a lightweight asynchronous memory access mechanism over the synchronous DDRx interface. Twin-load uses two special loads to accomplish one access request to extended memory — the first serves as a prefetch command to the DRAM system, and the second asynchronously gets the required data. Twin-load requires no hardware changes on the processor side and only slight software modifications. We emulate this system on a prototype to demonstrate the feasibility of our approach. Twin-load has comparable performance to NUMA extended memory and outperforms a page-swapping PCIe-based system by several orders of magnitude. Twin-load thus enables instant capacity increases on commodity platforms, but more importantly, our architecture opens opportunities for the design of novel, efficient, scalable, cost-effective memory subsystems.*

1. Introduction

Commodity memory interfaces have difficulty in scaling memory capacity to meet the needs of modern multicore and big data systems. For instance, the number of cores in chip multiprocessors (CMPs) is growing such that memory capacity per core drops by 30% every two years [36]. In virtualized environments, running many consolidated virtual machines per core further increases memory requirements [13]. Sufficient capacity to hold frequently used “hot” data becomes critical to avoid slow disk accesses. For example, the total memory used for data caching in Facebook is about 75% of the size of its non-image data [44]. In-memory databases can perform queries 100 times faster than traditional disk-base approaches [9, 22]. And Google, Yahoo, and Bing store their search indices entirely in DRAM [34].

This “capacity wall” has several causes. First, the number of channels is limited by the processor’s pin count, estimated to increase only by 6.5% each year [29]. Second, the DRAM channel connects multiple dual in-line memory modules (DIMMs) via a multi-drop bus. Signal integrity (SI) requires that higher-frequency bus supports fewer DIMMs per channel, e.g., the newest Intel Xeon only supports one dual-rank DIMM per channel for DDR3-1866 [27]. Third, it is challenging to scale DRAM feature sizes below 20nm [29, 43].

Buffer chips can be used to mitigate pin count and SI limitations [19, 18, 39], but the processor’s maximum tolerable access latency still restricts current solutions to one-layer extensions. This constraint can be avoided by accessing memory via packet-based asynchronous protocols [24, 49, 36, 38, 23]. For instance, standard PCIe can be used to access DRAM in remote servers [23] and disaggregated memory blades [36, 38], but random accesses to large working sets can suffer 100× slowdowns [23]. Asynchronous protocols can be implemented over high-speed serialized links [24] or photonics [49], but the expense has thus far limited their widely adoption. We believe that an industry-standard asynchronous interface is the right way to go, but any solution that requires changes to the processor interface slows commercial adoption.

We seek a practical solution to the capacity wall that is much more scalable, requires no changes to commodity processors and memory modules, and delivers acceptable performance for big-memory applications. We use Memory Extending Chips (MECs) to build a multi-layer memory system, the extra propagation delay for which violates DRAM latency constraints. To address this, each access to the extended memory is replaced by two special *twin-loads*, where the first one prefetches data into the MEC buffer, and the second one brings it into the processor. The twin-load addresses point to the same location, but we manipulate them so that 1) the second load reaches the MEC rather than hitting in cache and 2) the commodity processor is tricked into serializing them on the memory interface to ensure time to complete the prefetch.

Our contributions are:

- We implement an asynchronous protocol over the synchronous DDRx interface by introducing a twin-load mechanism that coordinates software and hardware.
- We propose to use commodity processors and memory modules to create a scalable extended memory system based on twin-load. We study two different mechanisms to guarantee

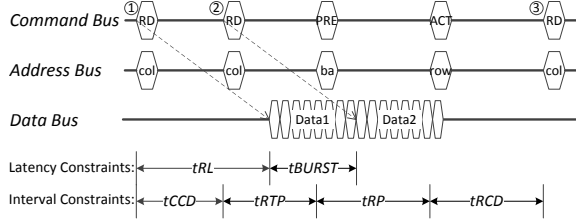


Figure 1: DRAM Access Protocol. RD ① and RD ② map to the same bank and row, while RD ③ maps to another row in that bank. The rank and bank addresses associated with each command are omitted for readability.

Table 1: DDRx Timing Parameters

Timing ^a Parameter	Description	Typical Value
t_{RL}	Fixed latency from RD command to first data	13.75ns
t_{BURST}	Fixed duration of data transfer	4 cycles
t_{CCD}	Minimum delay between two RD commands	4 cycles
t_{RTP}	Minimum delay between RD and PRE commands	7.5ns
t_{RP}	Minimum delay between PRE and ACT commands	13.75ns
t_{RCD}	Minimum delay between ACT and RD commands	13.75ns

^a Delays between commands to the same bank

prefetch-to-load order and enough time for the prefetch. One of them enables exploiting the memory concurrency.

- We implement a software prototype that reserves memory from the operating system to emulate the extended memory and MECs, and we implement a lightweight extended memory manager.
- We use our prototype to evaluate the feasibility of our proposals, finding that our best solution has comparable performance with NUMA extensions, but better scalability and performance per dollar. For applications with large working sets and irregular accesses, our twin-load solutions perform orders of magnitude better than page-swapping with PCIe-connected remote memory. Even when compared to an ideal system with all local memory, twin-load incurs an acceptable slowdown (about 26%).

The ability to quickly, easily, and inexpensively increase memory capacity delivers good return-on-investment, but it is not the most compelling benefit of our memory architecture. Rather, our approach opens new opportunities to build innovative, efficient memory systems such as integrating remote memory pools, heterogeneous DRAM/NVM, direct remote memory access, and even accelerators into the MECs.

2. Background and Related Work

DRAM memory systems usually consist of multiple channels that drive DIMMs composed of multiple ranks, and all ranks on a channel share a command, address, and data bus. A rank contains multiple storage arrays, or banks. Total memory capacity is thus determined by the number of channels, the ranks per channel, and the rank capacity, which are limited by the pin count, signal integrity, and chip density, respectively.

Simple synchronous protocols like JEDEC DDRx [31, 32]

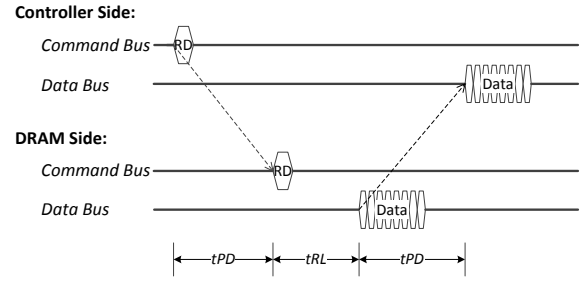


Figure 2: DRAM Access with Extending Hardware. t_{PD} is the propagation delay of commands/data between the memory controller and DRAM chips.

are commonly used to access the data arrays; in such protocols, data are placed on the bus a fixed latency after being requested, and thus no handshake occurs between the producer and consumer. An *activate* (ACT) command “opens” a given row, loading the target row’s data into a bank of sense amplifiers from which read (RD) and write (WR) commands access the data at specified columns. Subsequent accesses to an open row (*row hits*) require no ACT command to resend the row address. When data from a different row are needed (*row misses*), the memory controller sends a *precharge* (PRE) command to “close” the row, which writes the data back to the storage array and precharges the bank’s sense amplifiers. It then issues an ACT command to open the new row.

Figure 1 illustrates the basic operation, and Table 1 shows the related timing parameters. For example, RD ② in Figure 1 is a row hit. The ACT is omitted, and the RD can be issued after a short t_{CCD} latency. RD ③ is a row miss, and so a PRE command is sent after t_{RTP} time to close the row. After t_{RP} time to finish the precharge, an ACT command with the new row address is sent, and the RD command with the column address can finally be issued after t_{RCD} time.

2.1. Memory Extension over Standard DDRx Interfaces

Buffer chips can be used to alleviate pin count and SI constraints within the latency requirements of DDRx protocols. For instance, Cisco’s unified computing system extended technology uses an ASIC buffer to expand a DDR3 DRAM channel into four distinct channels [18], yielding up to $4\times$ the capacity. Such buffer chips with five DDRx interfaces become expensive due to large die area and packaging costs. LRDIMM uses a memory buffer to re-drive the DRAM bus, alleviating SI issues and enabling more DIMMs/channel [39]. Scalability is still limited at higher frequencies: e.g., at DDR3-1866 the newest Intel Xeon only supports one LRDIMM per channel [26].

Both methods have limited scalability because they can only support one-layer extensions. When extending hardware is interposed between the memory controller and DRAM chips, commands and data experience extra propagation delays. For DRAM writes, commands and data propagate in the same direction, remaining synchronous on the channel. DRAM reads require longer round-trip times because data and commands

move in opposite directions. Figure 2 shows the difference in read timing. For the simplest scenario where the extending hardware just forwards commands and data without any processing, the extra delay is $3.4ns$ in each direction [25]. The DRAM read latency in the memory controller, t_{RL} , can be increased by $6.8ns$, which is still within the adjustable range of commodity processors. For a slightly more complex system with two layers of extending hardware and minimal logic processing, the propagation delay will likely approach $20ns$, which is difficult for commodity processors to tolerate.

2.2. Memory Extension over Custom Memory Interfaces

There are many proposals for replacing the synchronous memory interface and breaking the tight processor-memory coupling. Typically, an interface buffer/die is introduced to bridge processor and memory, such as FBDIMM [30], BOB [19], and HMC [24]. Other researchers study more exotic organizations; for instance, Chen et al. [17] study a message-based memory subsystem with high-speed serial links; Fang et al. [21] incorporate emerging technologies on DDRx-like buses; and Udipi et al. [49] look at using 3D stacking and photonics to create scalable memory systems. The protocol between the buffer/die and memory is still a synchronous DRAM protocol, but the protocol between the buffer/die and processor is replaced by a packet-based access protocol. Although such methods are effective, they require changes to the memory controller and processor-memory interface. It is uncertain whether processor vendors will accept such solutions. Even if they do, high cost and increased access latency may still limit adoption, e.g., BOB is only supported in high-end product lines.

2.3. Memory Extension over Inter-Processor Interfaces

A coherent network can connect multiple server processors to form a NUMA (Non-Uniform Memory Access) node. Each processor can access memory on other nodes with additional latency, which extends the total capacity of directly addressable memory. Various NUMA systems are available from low-end, dual-socket systems to those with 100s of CPUs [48]. When it comes to memory capacity, though, NUMA is expensive. First, adding more memory modules necessitates adding more processors, which may be wasteful for memory-bound applications. Second, maintaining cache coherence across shared memory incurs significant overheads. Both complexity and cost are added to the processor, e.g., only high-end processors support NUMA with more than two processors. Third, the access latency across a NUMA interconnect is relatively high, e.g., the Intel Quick Path Interconnect (QPI) adds about $58-110ns$ latency per hop [42].

2.4. Memory Extension over Network Interfaces

PCIe is an asynchronous, packet-based protocol. The lack of a latency constraint facilitates the design of scalable DRAM organizations over standard PCIe interface, but the latency of accessing memory via PCIe is several microseconds. Lim et

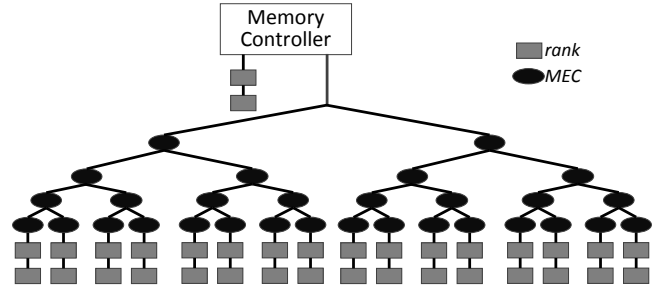


Figure 3: Four-layer tree topology, assuming that a channel can only drive dual ranks at high frequency [27]

al. [36, 38] find that page-swapping between local and remote memory via DMA performs reasonably for applications with high locality, but swapping is inefficient for applications with large working sets and irregular access patterns. Besides, data accessed via PCIe are not directly cacheable. Other proposals can use memory on remote servers or memory blades via a network interface. Software approaches like vSMP [12] and MemX [20] access memory on remote servers over commodity InfiniBand or Ethernet. For all I/O interface based schemes, the latencies are difficult to go below one micro-second.

2.5. Memory Extension with Emerging Technologies

Emerging storage class memory (SCM) technologies such as PCM and ReRAM could provide higher storage density and lower power consumption than DRAM at comparable access latencies, making it a potentially good candidate for capacity extension. However SCM has more timing constraints that are quite different with DRAMs. For example, write latencies are about $10\times$ longer than read latencies, and reads are still $2-3\times$ slower than DRAM [35]. So it is not possible to access SCM through the commodity DDRx SDRAM interfaces without modifying the processor-integrated memory controller. Micron recent PCM chip [41] uses a special JEDEC LPDDR2-N [33] interface that adds a PRACTIVE command and an overlay window especially designed for NVM. SanDisk's UltraDIMM connects NAND flash to CPU through DDR3 Interface but only supports direct access to internal buffer [11]. Since SCM technology is still evolving, it is unlikely that a universal interface will be well defined and adopted by processor community soon.

3. Overview

Both the DDRx and PCIe are widely-used, open standards, which makes their interfaces good candidates for memory extension. We choose the memory interface because of two advantages: latency and concurrency. Even with the extra propagation delay, the access latency to extended memory is still within tens of nanoseconds. And since these accesses are cacheable, non-blocking caches help mask delays.

Figure 3 illustrates one potential memory extension topology that allows us to populate more than two ranks per channel. The Memory Extending Chips implement one slave and

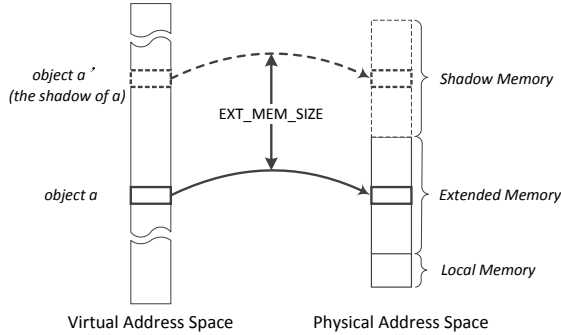


Figure 4: Relationship between virtual and physical memory spaces. The shadow space does not map to real DRAM.

one master DDRx interface. The slave of the *top-level MEC* (MEC1) connects to the processor’s commodity memory interface, and the master connects to the DIMMs or to the slave interfaces of other MECs. The MEC interfaces are similar to those of LRDIMM [18], but the internal logic and associated software break the one-layer constraint.

Since DRAM reads to extended memory experience intolerable round-trip times, we must access the data in a way that breaks the t_{RL} constraint. Note that both loads and stores cause DRAM reads. Stores first trigger read-for-ownership (RFO) operations to bring data into cache. They update the data in cache, and on eviction they write back to memory. We thus first discuss how loads work before discussing stores.

3.1. Load Operations

To break the latency constraint, we could first prefetch the target data into the buffer of MEC1 and insert a line of fake data (e.g., repetitive patterns of 0x5a) as a placeholder in the processor’s caches. A second demand load could then fetch the real data from the MEC. This scheme presents three challenges. First, we can neither issue two normal loads to the target address nor use a software prefetch instruction, since those would cause the demand load to hit in cache and load the placeholder data. The demand load must reach MEC1 to get correct data. Second, MEC1 must process the prefetch first. Modern processors typically employ out-of-order (OoO) execution in the instruction pipeline or the memory controller queue, which makes the order in which the loads reach the MEC unpredictable. Third, the MEC must issue the prefetch early enough to guarantee that the data will be loaded into its buffer before the demand load fetches the data.

To address the first challenge, we manipulate the data addresses so that the processor thinks the prefetching load is to a different location from the demand load, but the MEC knows that they correspond to the same target location. For instance, adding a flag bit suffices to distinguish the addresses inside the processor. The MEC simply ignores this bit. This creates a “shadow” address for each location in the extended memory. Figure 4 shows the relationships among the local, extended, and shadow memory spaces.

To address the second and third challenges, we design two different twin-load mechanisms. We also investigated an extreme way to guarantee strong ordering by making the extended memory uncacheable [28], but we omit those results here due to its poor performance.

The first mechanism, **TL-LF**, inserts a *load fence* instruction between the loads. The fence guarantees that the second load will not execute until the first receives data from memory [28]. The spacing between the loads is the round-trip time of a memory load, which is large enough to tolerate the propagation delay. This mechanism retains the benefit of cache locality, but blocks all loads following the fence.

To better exploit memory concurrency, we need to allow more out-of-order execution. Our second solution, **TL-OoO**, does not designate which is the prefetch or demand load at the software level, but assigns appropriate identities dynamically via both hardware and software. The load that arrives first triggers the prefetch and returns fake data, and the one that follows returns the true data. Software identifies which data is correct on-the-fly.

If both the extended and shadow addresses map to the same DRAM bank, the second twin-load artificially triggers a DRAM row miss that forces TL-OoO to delay the load’s MEC arrival. Recall that an RD command to the same bank but different row must wait t_{RTP} time before issuing the PRE to close the current row, t_{RP} time to complete the PRE and issue the ACT for the new row, and finally t_{RCD} time to complete the ACT and issue the RD. The minimum total delay is about 35ns at DDR3-1600, which is enough to tolerate propagation delays for up to five MEC layers.

3.2. Store Operations

We need twin-loads to bring data into cache before we perform store operations. Memory consistency requires us to ensure that data always be written to the true cache line. In the unlikely event that an interrupt happens between the twin-load and the store, the correct cache line may have been evicted by the time the store is resumed. The store has to trigger an RFO operation to load a fake line into cache, the modification of which will cause an error. To avoid this, an atomic *compare_and_swap* (CAS) instruction¹ first compares the correct value obtained from the twin-load with the value in the cache line, and swaps (stores) the new value into the cache line only when the comparison succeeds. Then if the RFO after the interrupt brings the fake data into cache, the comparison will fail, the cache line remains unmodified, and the store is retried.

4. Implementation Details

The MECs organize the physical DIMMs/ranks/banks into logical DIMMs/ranks/banks that the memory controller sees. MEC1 asserts a fake serial presense detect (SPD) [40] to the memory interface, and all MECs maintain simple mapping

¹CAS is named CMPXCHG in the x86 instruction set [28].

Original Code: <code>val = *p;</code> Replaced by: <code>val = load_type(p);</code>	Original Code: <code>*p = val;</code> Replaced by: <code>store_type(p, val);</code>
<pre> type load_type(type *p1) { type v1, v2; type *p2=(void*)p+EXT_MEM_SIZE; v1=*p1; v2=*p2; if(v1 != FAKE_VALUE) return v1; else if(v2 != FAKE_VALUE) return v2; else return retry_load_type(p); } </pre>	<pre> void store_type(type *p1, type newval) { type v1, v2; type *p2=(void*)p+EXT_MEM_SIZE; v1=*p1; v2=*p2; if(v1 != FAKE_VALUE) if(!type_cas(p1, v1, newval)) retry_store_type(p1, newval) else if(v2 != FAKE_VALUE) if(!type_cas(p2, v2, newval)) retry_store_type(p1, newval) else retry_store_type(p1, newval); } </pre>

Figure 5: Semantics of twin-loads in TL-OoO

tables. MEC1 chooses one address bit to differentiate the extended and shadow memories. For TL-OoO, that bit must be a row address bit, and since memory controllers generally use the most significant bit (MSB) of the physical address in the row address, we choose it. For simplicity, TL-LF also uses the MSB, even though it affords more flexibility in how memory capacity grows. The physical memory space consists of the local memory, extended memory, and shadow memory. Figure 4 shows that only local memory and extended memory physically store data.

4.1. Software Modifications

The programmer must identify which objects to place in extended memory. Large data objects make good candidates, whereas the OS, code, stack, and small objects should be in local memory. The programmer use a special interface to allocate objects in extended memory. For the most complicated application we evaluate, the modifications took less than two days (including time to understand the code). For applications that index large arrays to access data, they took less than half a day.

Figure 5 shows how loads and stores to identified objects in the program are replaced by (inlined) functions that implement TL-OoO. Loads to virtual address p are replaced by the function $load_type(p)$, which loads both p and p' concurrently, and compares their return values to identify the correct one. Stores to virtual address p are replaced by the function $store_type(p, val)$. Two functions, $retry_load_type(p)$ and $retry_store_type(p, val)$, handle the cases in which both loads return fake values or the atomic CAS fails.

Such modifications can be done automatically by a compiler with user-annotations. This work will be introduced in our future paper.

4.2. Extended Memory Management

Modifying the OS is a practical means of managing the extended memory, but for this study we choose to implement a lightweight manager outside the OS. Big memory applications usually allocate most memory during initialization, with few changes to the allocations throughout execution [15, 45]. For

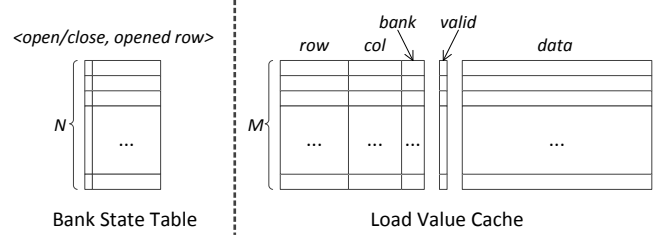


Figure 6: The Bank State Table and Load Value Cache in the MEC1 hardware. N and M are the number of entries, respectively, where N is equal to the number of logical banks, and M is a design parameter.

example, Memcached [5] preallocates a big chunk of memory at startup and self-manages it to allocate items internally. Such applications need no complex managers to minimize fragmentation due to frequent allocations and deallocations.

The extended and shadow memory spaces are reserved by the OS at boot time and can be allocated in user space via $mmap()$. To simplify memory management, we allocate/deallocate extended and shadow memory together in large blocks (e.g., 64MB). When allocating a block, two virtual memory regions at a distance of EXT_MEM_SIZE are allocated, as well. Both the virtual and block physical addresses are passed to two $mmap()$ calls to construct corresponding virtual-to-physical mappings in the page table. If the virtual address of an object in extended memory is p , the corresponding virtual address for its shadow p' is simply $p+EXT_MEM_SIZE$, as shown in Figure 4.

4.3. Twin-Load Processing

In a multi-layer extended system, MEC1 identifies the two loads and forwards the request on the first load, temporarily buffers the data, and returns it on the second load. The MECs on the other layers are much simpler, either executing the received commands or forwarding them to the next layer.

MEC1 maintains two main structures not required in lower MECs: the Bank State Table (BST) and the Load Value Cache (LVC), illustrated in Figure 6. The routing table required to implement tree topologies is not shown. For each logical bank, a BST entry indicates whether the bank is open and stores the address of the last row opened. The LVC entries temporarily store prefetched values for the first loads. The tag is the address, and the valid bit indicates whether the entry is in use. Our LVC uses LRU replacement.

Upon receiving an ACT command, MEC1 records the bank's row address in the BST. When the RD arrives with its bank address, the MEC accesses the BST to retrieve the previously issued row address. The load address is reconstructed as $\langle row, column, bank \rangle$.

For TL-OoO, the address is the tag for the LVC lookup: if the lookup misses, the access should be the first load, otherwise the second load. When MEC1 sees the the first load, it allocates an LVC entry, sets the tag to the load address, sets

Table 2: Twin-Load Results with Respect to Cache State

State	v	v'	DRAM Reads	Result
1	not in cache	not in cache	two	v, v'
2	in cache	in cache	zero	v, v'
3	in cache	not in cache	one	v, v'
4	not in cache	in cache	one	v', v'

the valid bit, and forwards the RD to the target MEC. After t_{RL} time, it puts the fake values on the data bus to the memory controller. The target MEC fetches the data from DRAM and returns it to MEC1 with the LVC entry ID, where it is inserted into the MEC1 LVC.

In general, the LVC size M should try to guarantee that the corresponding entry will not have been evicted when the data return, i.e., $M > (2 \times t_{PD} + t_{RL}) / t_{CCD}$, where $2 \times t_{PD} + t_{RL}$ is the round-trip time for returning data, and t_{CCD} defines the minimum interval between consecutive RDs. For TL-OoO, the maximum tolerable propagation delay is 35ns, and thus $M > 10$ suffices. TL-LF can tolerate much longer delays, and so the LVC must be larger. When MEC1 identifies the RD as the second load, it returns the data to the memory controller after t_{RL} time. The valid bit is cleared to free the entry.

If the second load arrives too late, the data may have been evicted from the MEC1 LVC. For TL-LF, the second load then returns the fake value. For TL-OoO, the MEC will identify the intended second load as the first, reallocate a new cache entry, return fake values, and prefetch the data again. Software retry ensures that the load gets correct data, but we want to avoid such cases, which waste prefetches and hurt performance. By monitoring our prototype’s DRAM command bus, we find that twinned loads are separated by an average of six other loads, which can guide the design choice of M .

The middle MECs forward commands to the target leaf MECs to execute. They use the high bits of the row address as the physical DIMM ID for command forwarding. The routing table determines the forwarding port. For the ACT command, the ID is in the row address. For other commands, MEC1 gets the ID from the BST and passes it with the command.

4.4. Cache State and Correctness

Since both extended and shadow memory are cacheable, one or both of the twin-load accesses might not reach MEC1. Let v be the correct value and v' the fake value. Table 2 lists their possible states with respect to the cache. In State 1, the initial state, both loads trigger DRAM reads. The MEC takes the first read as the prefetch and returns the fake value and then returns the correct data on the second read. In State 2, the MECs are not involved. Both loads commit quickly, one with the correct value and one with the fake value. In State 3, one load returns the correct value directly from cache, and the MEC identifies the other load as the prefetch and returns the fake value. The corresponding LVC entry will eventually be evicted. In State 4, one load hits in cache and returns the fake value, and the other causes a DRAM read that *also* returns the fake value,

since no former prefetch has reached the MEC.

We fall back to a software retry to handle this case: both load addresses are first invalidated to return to state 1, and then we use another twin-load to get the correct data. A memory fence instruction is required to complete the invalidation before the following twin-load. If the retry also gets the fake value, we throw an exception that invokes a safe path to memory. We are investigating other strategies for better performance, but discussing them is beyond the scope of this paper.

4.5. Exception Handling

There are two rare cases in which the retry may fail: the LVC entry gets evicted before the second load arrives, or the correct data is the same as the fake value. Our solution is to implement a slow but safe path by which to load the data. We add three uncacheable memory mapped registers in MEC1: an address register to receive the physical load address, a flag register to indicate load completion, and a data register to hold the loaded data. The exception handler actions are like reading I/O ports.

5. Evaluation Methodology

To evaluate our twin-load implementation, we emulate multiple systems for comparison:

- TL-LF and TL-OoO: our twin-load mechanisms with local, extended memory, and shadow memory;
- NUMA: a system using QPI to connect more processors so they can attach more memory;
- PCIe: a system using PCIe to connect more memory, which is accessed using page swapping [36, 38]; and
- Ideal: an ideal system with all memory locally attached.

Our host system has two processors and eight 8GB DIMMs (64GB in total). Table 3 shows how the host memory is used to emulate the extended memory systems. For the TL, PCIe, and Ideal systems, we attach all DIMMs to a single processor (and execute only on that processor) to avoid performance variations among different runs due to nondeterministic memory-to-processor affinities. Our experiments are independent of any specific topology — as long as the propagation delay in within 35ns, the software behaves the same.

For the TL systems, both the extended and shadow memories are emulated using reserved host memory. The shadow memory is initialized to hold fake values to emulate the MEC functionality. The twinned addresses cause DRAM row misses in the host memory controller. We implement the required

Table 3: Emulated Systems

System	TL	NUMA	PCIe	Ideal
Processor	One Intel Xeon E5-2640 Processors (6-core, 12-thread) ¹			
Local Memory	0-8GB		0- x GB ²	0-32GB
Extended Memory	8-32GB		x -32GB ²	-
Shadow Memory	40-64GB		-	
Extended Interface	DDR _x	QPI	PCIe	-
Access Mechanism	TL-LF/TL-OoO	cc-NUMA	Swapping	Ideal

¹ We have two processors, but use only one for program execution for all systems.

² We vary the cut-off point to emulate different local:swapped ratios.

Table 4: Workloads

Benchmark	Source	Type	Description	Proportion in extended memory
GUPS	HPC Challenge [2]	Micro-Benchmark	Random access	100.00%
Radix	PARSEC3.0 [10]	Kernel	Integer sort	100.00%
CG	NPB2.3 [7]	Scientific Computing	Calculating conjugate gradient	99.43%
FMM	PARSEC3.0 [10]		N-body simulation	94.39%
BFS	Graph500 [1]	Graph Application	Breadth-first search	99.79%
BC	SSCA2.2 [3]		Calculating connection centrality	76.92%
PageRank	In-house implementation		Calculating website ranks [16]	87.93%
ScalParC	NU-MineBench [8]	Data Mining	Parallel classification	94.48%
StreamCluster	PARSEC3.0 [10]		Online clustering	92.93%
Memcached	Memcached-1.4.20 [5]	Data Serving	Key-value caching system	97.30%

software to generate twin-loads to the extended and shadow memories for certain accesses. For the NUMA systems, we attach one DIMM to one processor to emulate local memory and attach seven DIMMs to the other processor to emulate extended memory. Programs execute on the former and access extended memory via QPI. For the PCIe system, we emulate extended memory as a host-memory RAM Disk configured as a swap partition. We emulate the remote page swapping with default Linux swapping to the RAM Disk. For the Ideal system, we emulate all local memory as host memory. No software change is required.

Note that there are some deviations between a real twin-load system and the emulated system. In the emulated system:

1. loads to the extended and shadow memories always return the correct and fake values, respectively, thus it is possible that the correct value returns earlier and advances program prematurely; and
2. for the fourth case in Table 2, the missed load always returns the correct value from memory, whereas it should return the fake value and trigger a retry.

To avoid the first situation, we choose to advance the program only when both the values have been returned and checked. This is a conservative choice, since for the first and third cases in Table 2, it could be that the correct value in cache is compared first, and the program could proceed without waiting for the result of another load. It is difficult to avoid the second situation because the software cannot know the cache state. However, by recording the memory requests on the memory bus using a tool like a DDR3 protocol analyzer [4], we find that over 96% of loads to extended memory are twinned. This can be easily explained, since the two addresses are always accessed synchronously and are very likely to be brought into and evicted from cache together. Taking into account the conservative policy for the first deviation, we believe our emulation reasonably approximates a real extended system.

Table 4 lists the workloads we use in our evaluations. From a variety of application domains, we select 10 benchmarks with footprints that scale easily and code sizes that are reasonable for manual modification. For Memcached, a client running *memslap* [6] is connected to the Memcached server via Gigabit Ethernet; to avoid the network bandwidth becoming bottleneck, we test small objects [37] and only use four

threads on the server side.

For all benchmarks, we evaluate two footprints — a medium one around 4GB and a large one around 16GB. For the TL and NUMA systems, we modify source code to allocate large objects in extended memory. Table 4 shows the proportion of data in extended memory. For the PCIe system, we let the Linux swap mechanism manage data placement. We use performance counters to gather architectural statistics.

6. Results

We compare TL-LF and TL-OoO against the NUMA and Ideal systems described in Section 5. Figure 7 shows experimental results for these mechanisms on our emulated prototypes. We normalize performance relative to Ideal. TL-LF, TL-OoO, and TL-NUMA achieve 45%, 75%, and 73% of Ideal performance for medium footprints, and 49%, 74%, and 76% of Ideal performance for large footprints. This suggests that footprint size does not significantly affect performance, so we restrict our discussion to large-footprint results.

6.1. TL vs. Ideal

We first discuss the potential penalties for twin-load compared to having all local memory. Then we discuss how TL-OoO might alleviate certain penalties. Finally, we discuss the shortcomings of TL-LF and discuss future optimizations.

Potential Penalties. Twin-load obviously increases the number of instructions and data accesses, potentially causing more cache misses. Also, since we double the address space, TLB conflicts will be exacerbated. Figure 8, Figure 9, and Figure 10 show the effects of twin-load on instruction execution, LLC, and TLB behaviors. (Note that the LLC MPKI and TLB MPKI of TL-OoO are relative to the number of retired instructions in the Ideal case, to show the absolute miss increase.) Since twin-load replaces some load/store instructions with inline functions, the increase in number of instructions retired depends on the proportion of memory accesses and their relative proportion targeting extended memory. TL-OoO’s retired instruction count increases by 64%, on average. LLC misses increase by 11-156% (71%, on average). If all data are in extended memory, the number of LLC misses can potentially double, as is the case for GUPS, Radix, CG, and BFS. For others (e.g., BC, PageRank, and ScalParC) a small portion

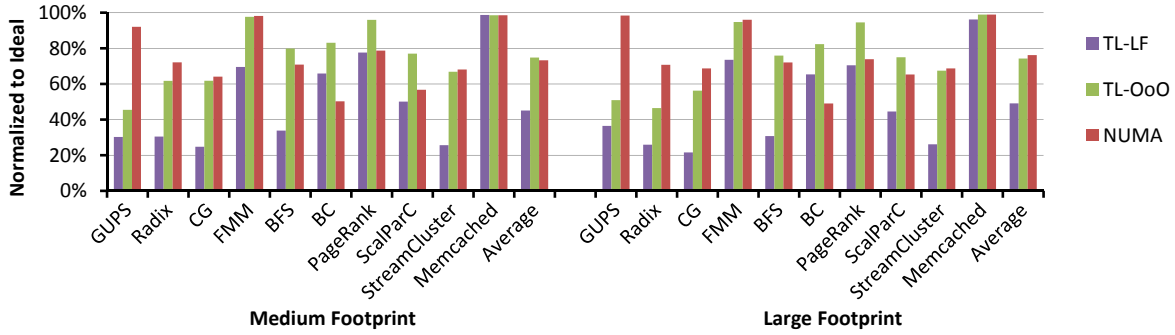


Figure 7: Normalized Performance of Various Mechanisms

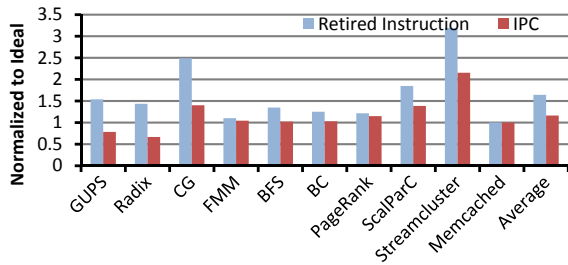


Figure 8: Instruction Count and IPC of TL-OoO Relative to Ideal

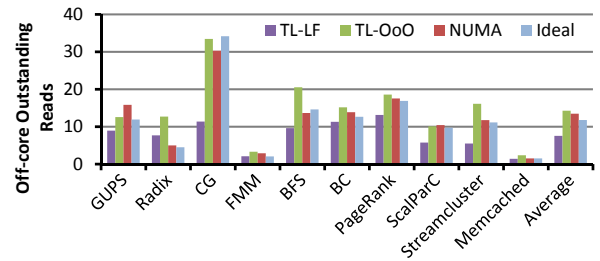


Figure 11: Average Number of Off-Core Outstanding Reads

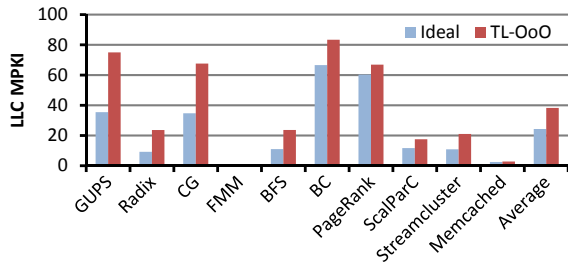


Figure 9: LLC MPKI

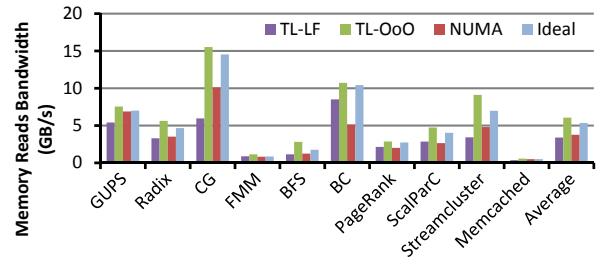


Figure 12: Average Read Bandwidth

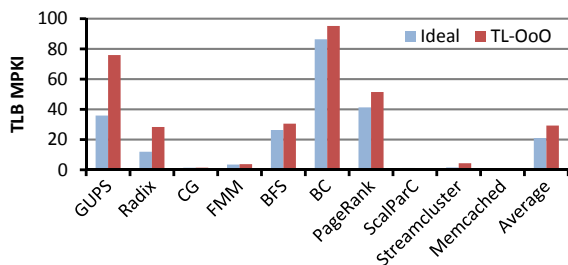


Figure 10: TLB MPKI

of local data may contribute to a significant portion of the accesses, thus twin-load only modestly increases LLC misses.

Figure 10 shows that workloads with significant TLB conflicts can be classified into two categories: graph applications and applications that store most data structures in extended memory. For instance, doubling the extended address space roughly doubles the TLB misses for GUPS and Radix. For the graph applications, our results suggest that the relative small but frequently accessed vertex-associated metadata (rather than the large graph) contribute to most of the TLB misses.

This is because such metadata are randomly accessed and large enough to exceed the TLB coverage (2MB for a 512-entry TLB with 4KB pages), and the graph traversal thrashes the TLB. Workloads with relatively good locality (e.g., CG and ScalParC) cause few TLB conflicts. Increases in TLB MPKI range from 3% to 179% (39% on average).

Potential Benefits for TL-OoO. Although twin-load increases the number of executed instructions by 64% and LLC misses (long latency memory accesses) by 71% compared to Ideal, average performance slowdown for TL-OoO is only 25% and 26% for medium and large footprints, respectively. This is due to twin-load's better processor utilization: Figure 8 shows that even though twin-load increases the number of instructions, it delivers higher IPCs for most workloads. (The remaining gap reflects the performance slowdown.) The pipeline usually stalls on long-latency memory accesses, but our twin-load instructions can exploit such stall slots, masking the increase in non-memory instructions.

Achievable memory-level parallelism (MLP) of most applications is limited, which is far from saturating the processor's available memory access concurrency, which is defined by the

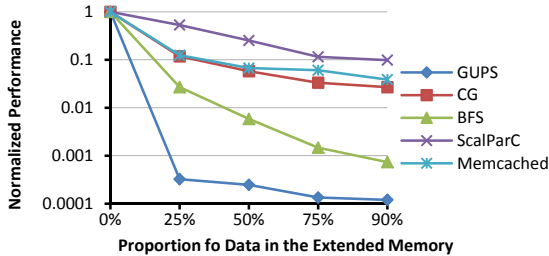


Figure 13: Performance of PCIe Swapping mechanism

number of MSHRs. Thus TL-OoO can take advantage of the remaining capacity for concurrency to overlap execution of the extra loads. Figure 11 shows that the average number of outstanding off-core reads increases from 11.8 to 14.3, especially for those workloads with significant increases in LLC misses (except GUPS and CG). GUPS’s concurrency is likely limited by the many TLB misses, while CG seems to saturate the hardware support for concurrency. Since we increase memory concurrency, the achievable memory bandwidth also increases, as shown in Figure 12.

Shortcomings of TL-LF. The most obvious shortcoming of TL-LF is its limited memory concurrency. Consecutive accesses to extended memory are serialized by the load fence. Figure 11 and Figure 12 show that the number of outstanding off-core reads and the memory read bandwidth are both decreased by 34%. Although it incurs more than 50% slowdowns, TL-LF can potentially tolerate higher latencies than TL-OoO, making it adaptable to more application cases. A possible optimization for TL-LF is not to insert a fence per data access, but to batch the first twin-load instructions for several accesses, insert the fence, and then perform the second twin-loads and software checks. We leave this for future work.

6.2. TL vs. NUMA

Figure 7 shows that TL-OoO exhibits comparable performance to NUMA. On our host system, the access latency to local memory and remote memory (via QPI) is about 100ns and 170ns, respectively. For NUMA, the long latency to extended memory and the limited memory concurrency cause memory throughput (bandwidth) to decrease by an average of 30% (and up to 51%) compared to Ideal, resulting in an average 24% (and up to 51%) performance slowdown. TL-OoO performs much better than NUMA for graph applications, in particular. The irregular access behaviors and corresponding limited intra-thread memory concurrency make graph applications latency-sensitive. Compared to the 70ns latency increase for NUMA, TL-OoO incurs less relative penalty — recall that a row miss causes only 35ns extra latency.

6.3. TL vs. PCIe

We evaluate the performance slowdown of using PCIe extended memory paging. In the experiment, we change the ratio of data to be placed on extended memory, ranging from

0% to 90%. The original replace procedure in Linux is designed for swapping with much slower hard disk so that it may be quite complicated and slow for swapping with fast PCIe remote memory. It takes about 7.8us to swap a page on our prototype, which is 1.4× of the fastest PCIe replacement policy [38]. Thus, to compensate for such extra software overhead, we double the measured performance of the emulated PCIe system in the comparison result. We choose five representative benchmarks — GUPS, CG, BFS, ScaleParC, and Memcached — from Table 4.

Figure 13 shows results normalized to those of a non-swapping (0% data in extended memory) system. Placing only 25% of data into extended memory slows performance of most workloads by quite much. Performance further degrades as we move more data into extended memory. At 90%, swapping pages with PCIe extended memory yields slowdowns of one to four orders of magnitude.

When 25% of data reside in extended memory, ScalParC has the best performance (0.53×), mainly due to its low LLC and TLB MPKIs, which suggest good locality and less pressure on the memory system. The extremely random-access GUPS only achieves 0.0003× the performance. Even for Memcached, which shows insensitivity to the memory system (Figure 7), performance is only 0.13×. For CG and BFS, resulting performance is 0.12× and 0.27×, respectively. TL-LF and TL-OoO perform much better than this, even if we put over 90% of data into extended memory.

7. Discussion

We recognize that accurate cost projections can be difficult, we nonetheless try to put relative costs in perspective before examining the impact of extending the DRAM *tRL* time.

7.1. Cost Analysis

We compare three ways to extend memory capacity: TL coordinates software and MECs, NUMA adds more processors, and Cluster adds more servers. The PCIe scheme experiences

Table 5: Costs of various memory extension mechanisms

Costs	Baseline	TL-OoO	NUMA	Cluster
Processor ¹	2×\$1166/3	2×\$1166/3	4×\$3616/3	4×\$1166/3
Memory ¹	8×\$175/3	16×\$175/3	16×\$175/3	16×\$175/3
Motherboard and Disk ¹	\$1000/3	\$1000/3	1.5×\$1000/3 ²	2×\$1000/3
MEC ¹	-	8×100/3	-	-
Server power ³	\$252	1.3×\$252	1.8×\$252	2×\$252
Other costs	\$1325	\$1325	1.5×\$1325 ⁴	2×\$1325
Total Costs	\$3154	\$3963	\$8696	\$6308
Potential Speedup	1	x	2× x	2× x
Correction Factor	$c = 1$	$c = 0.74$	$c_1 = 0.76$ c_2 varies	c varies

¹ We assume a lifetime of three years.

² More processors require a larger motherboard.

³ Processors and memory contribute 50% and 30%, respectively to server power.

⁴ Servers with more processors take more space, increasing data center costs.

such slowdowns that we exclude it here.

Cost Model. The baseline system has two processors, which is the most cost-effective configuration, but it only supports one dual-rank RDIMM per channel (a currently common situation at higher frequencies and a likely continuing trend). We choose Intel’s mid-end Xeon E5-2650v2 processor with four memory channels and 16GB RDIMM for our comparisons. Our baseline system has 128GB memory in total.

We take costs of server components from the Intel and Amazon websites. We derive other costs from Barroso and Hölzle [14] — the server cost of a three-year amortization and cost of server power take 50% and 8% of the TCO (total cost of ownership) for a datacenter with mid-end servers². Other costs include capital outlay and operating expenses. Note that for NUMA systems, we must use more expensive processors that support four cores (here Xeon E5-4650v2).

We expect that the MEC costs about the same as the LRDIMM buffer, since both contain two DDRx interfaces. The die area of such a chip is mainly determined by pin count, rather than logic. We only add a table and a cache with tens of entries, and thus we do not consume much logic. We conservatively assume such a MEC costs \$100.

Performance Model. We assume that by doubling the memory capacity, performance can at most be improved by a factor of x . This factor can be quite large in certain cases: Graefe et al. [22] find $x \approx 100$ when the extended memory capacity can cover an in-memory database’s datasets. NUMA and Cluster also double the number of processors, so ideal speedup would be $2 \times$. However, each method brings certain penalties. Our results in Section 6 shows that TL and NUMA achieve 74% and 76% of Ideal performance due to twin-load software and long latency memory accesses. In addition, NUMA and Cluster also face the challenge of efficient parallelization. For applications that are difficult to distribute, e.g., graph applications, the penalty for the Cluster method can be large.

Performance per Dollar. Table 5 shows the potential speedups/slowdowns and costs of doubling memory capacity for the three systems. The table shows that relative performance per dollar among the mechanisms has no relation to x but rather to the correction factor c due to twin-load software, cross-processor access latency, or efficiency of parallel implementation. Figure 14 draws the performance per dollar relative to the parallel efficiency. TL can improve performance per dollar by at least 7% compared to NUMA when doubling memory capacity. At the meantime, TL has the better scalability: the standard Intel solution only supports up to eight processors, which limits the system to $4 \times$ the memory capacity. Clustering has better scalability with respect to memory capacity, but it is difficult to scale performance. TL outperforms Cluster whenever the distributed application achieves below 60% of Ideal performance, which is a challenge for many applications.

² Server amortization costs 29.5% (65.9%) of TCO for a datacenter with low-end (high-end) servers, and server power costs represent 14.3% (3.8%).

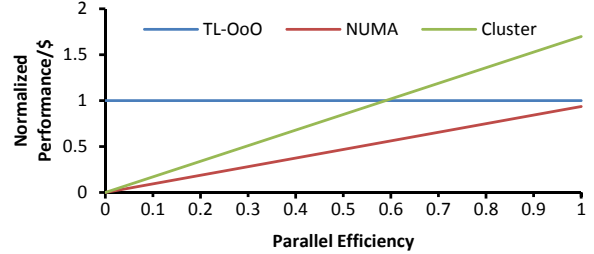


Figure 14: Normalized performance per dollar relative to TL-OoO.

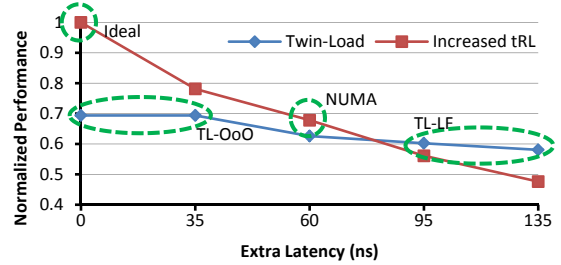


Figure 15: Simulated Results of TL vs. Increased t_{RL} (normalized to $t_{RL}=15ns$ without TL)

7.2. Comparison with Increased t_{RL}

To support the larger latency of extended memory, why not just increase the maximum latency constraint of JEDEC standard? Since t_{RL} , which determines data transmission time from memory chip to memory controller can be increased, the JEDEC DDRx standard could also adapt to extended memory with larger latencies. Although this scheme needs a tiny modification to memory controller hardware, it is still acceptable. However, according to the DRAM protocol, a memory bank will also be held for a longer time, preventing other accesses to that bank. This reduces memory bus concurrency, which reduces the benefit of this potential approach.

We compare TL extended memory to one using a single load with increased read latency. We use trace-driven DRAMSim2 [46] with dependences between memory instructions [47] to simulate the systems, and we choose more benchmarks than just those in Table 4. In the TL system, t_{RL} remains unchanged, but we insert a second load after each read to cause a row miss. To support latencies greater than $35ns$, the second load is delayed for certain time, but does not block following loads with no data dependence³. We compare extra latencies to tolerate of 0-135ns.

Figure 15 summarizes results. The four mechanisms from Section 6 correspond to special points in the figure and have coincident results expected for TL-LF. TL-LF tolerates latencies greater than $100ns$, but results on our emulated prototype are worse than in simulation, mainly because we simulate a TL mechanism that does not fence the following loads. In general, increasing t_{RL} performs better for relatively small

³ We assume such a mechanism can be realized by manipulating the instruction orders in software.

latencies, but as t_{RL} grows, performance degrades faster than for TL because high t_{RL} values limit memory concurrency. In contrast, the interval between twinned loads can be used to execute other memory requests.

7.3. Comparison with LRDIMM

Load-Reduced DIMMs are already used to maximize the server memory capacity. For example the newest Intel two-socket Xeon E5 server can support up to 1.5TB memory with LRDIMMs, if not considering the cost.

In fact, every buffer-based approach (including MEC) can be considered as reducing the electrical load. However, each buffer is typically capable of 2~4X load reduction, related to frequency. The real limitation of LRDIMM is one-layer extension, restricted by CPU's synchronous DRAM interface and access protocol – to be specific, the propagation of more layers violate CPU's timing constraint. To the best of our knowledge, commodity processors don't support cascading of LRDIMM buffers. Our proposal breaks such limitation towards more layers and much larger memory capacity using software supports, while LRDIMMs still can be used as local memory or extended memory after MEC.

Since LRDIMM has to put all memory chips within single level, the highest LRDIMM model already uses DDP (Dual-Die-Package) or QDP (Quad-Die-Package), or even 3DS devices. It is not surprised that a single LRDIMM is more expensive than a server CPU. While for multi-level MEC extension, more cost-effective RDIMM modules can be incorporated to build a large memory system.

7.4. Energy

The software overheads of twin-load would increase the energy consumption compared to the ideal system. For example, the retired instructions of TL-OoO are 1.64X that of ideal system, indicating more energy consumption. However, when compared to a real commodity system, the potential performance improvement due to twin-load enabled in-memory processing (up to 100X [22]), can actually greatly reduce the total energy consumption (Energy = Power \times Delay).

8. Conclusions

We propose twin-load, a mechanism to build a lightweight, asynchronous data-access protocol that requires no hardware changes on the processor side. To achieve this, we coordinate software and the Memory Extending Chips on a standard DDRx interface. Data access is accomplished by two special loads, the first of which prefetches data into the top MEC buffer and the second of which brings it into the processor. Using this mechanism, we can easily attach a multi-layer memory system to commodity processors to instantly address the capacity wall problem. We create an emulation-based software prototype to demonstrate the feasibility of our proposal. Our best mechanism can achieve 74% of the performance

of an ideal system with all local memory. Our mechanism performs similarly to NUMA extended memory, but delivers much better scalability and performance per dollar. Twin-load also outperforms PCIe-based systems by several orders of magnitude.

In addition to facilitating easy, cost-effective memory extensions, our mechanism opens opportunities to build innovative memory systems on commodity platform using the low-latency, high-concurrency standard DDRx interface; examples include remote memory pools, heterogeneous DRAM/NVM systems, direct remote memory accesses, and even MECs with integrated accelerators. Relying on open standards and avoiding changes to processor interfaces enables more system designers – including those in academia – to build production-quality systems.

References

- [1] "The graph500 list," <http://www.graph500.org/>.
- [2] "HPC challenge benchmark," <http://icl.cs.utk.edu/hpcc/index.html>.
- [3] "HPCS scalable synthetic compact applications #2 graph analysis," <http://www.graphanalysis.org/benchmark/index.html>.
- [4] "Kibra 480 analyzer," <http://teledynelecroy.com/protocolanalyzer/protocoloverview.aspx?seriesid=398>.
- [5] "Memcached - a distributed memory object caching system," <http://memcached.org/>.
- [6] "memslap - load testing and benchmarking a server," <http://docs.libmemcached.org/bin/memslap.html>.
- [7] "NAS parallel benchmarks," <http://www.nas.nasa.gov/publications/npb.html>.
- [8] "NU-Minebench," <http://cucis.ece.northwestern.edu/projects/DMS/MineBench.html>.
- [9] "Oracle unveils big memory machine to support in-memory databases," <http://www.serverwatch.com/server-news/Oracle-unveils-big-memory-machine-to-support-in-memory-database.html>.
- [10] "The PARSEC benchmark suite," <http://parsec.cs.princeton.edu/parsec3-doc.htm>.
- [11] "ULLtraDIMM SSDs," <http://www.sandisk.com/enterprise/ulltradimm-ssd/>.
- [12] "Versatile SMP (vSMP) architecture," <http://www.scalemp.com/technology/versatile-smp-vsmp-architecture/>.
- [13] "VMware to increase consolidation ratio to 16 VMs / core ?" <http://virtualization.info/en/news/2010/01/vmware-to-increase-consolidation-ratio.html>.
- [14] L. A. Barroso, J. Clidaras, and U. Hözlze, "The datacenter as a computer: an introduction to the design of warehouse-scale machines," *Synthesis Lectures on Computer Architecture*, vol. 8, no. 3, pp. 1–154, 2013.
- [15] A. Basu, J. Gandhi, J. Chang, M. D. Hill, and M. M. Swift, "Efficient virtual memory for big memory servers," in *Proceedings of the 40th Annual International Symposium on Computer Architecture*, 2013.
- [16] S. Brin and L. Page, "The anatomy of a large-scale hypertextual web search engine," *Computer networks and ISDN systems*, vol. 30, no. 1, pp. 107–117, 1998.
- [17] L.-C. Chen, M.-Y. Chen, Y. Ruan, Y.-B. Huang, Z.-H. Cui, T.-Y. Lu, and Y.-G. Bao, "MIMS: Towards a message interface based memory system," *Journal of Computer Science and Technology*, vol. 29, no. 2, pp. 255–272, 2014.
- [18] Cisco, "Cisco unified computing system extended memory technology overview," http://www.cisco.com/c/en/us/products/collateral/servers-unified-computing/ucs-b-series-blade-servers/white_paper_c11-525300.html.
- [19] E. Cooper-Balis, P. Rosenfeld, and B. Jacob, "Buffer-on-board memory systems," in *Proceedings of the 39th Annual International Symposium on Computer Architecture*, 2012.
- [20] U. Deshpande, B. Wang, S. Haque, M. Hines, and K. Gopalan, "MemX: Virtualization of cluster-wide memory," in *Proceedings of the 39th International Conference on Parallel Processing (ICPP)*, 2010.

- [21] K. Fang, L. Chen, Z. Zhang, and Z. Zhu, "Memory architecture for integrating emerging memory technologies," in *Proceedings of the 2011 International Conference on Parallel Architectures and Compilation Techniques (PACT)*, 2011.
- [22] G. Graefe, H. Volos, H. Kimura, H. Kuno, J. Tucek, M. Lillibridge, and A. Veitch, "In-memory performance for big data," *Proceedings of the VLDB Endowment*, vol. 8, no. 1, 2014.
- [23] R. Hou, T. Jiang, L. Zhang, P. Qi, J. Dong, H. Wang, X. Gu, and S. Zhang, "Cost effective data center servers," in *2013 IEEE 19th International Symposium on High Performance Computer Architecture (HPCA)*, 2013.
- [24] Hybrid Memory Cube Consortium, "Hybrid Memory Cube Specification 1.0," 2013.
- [25] Inphi, "imb02-gs02, imb02-gs02a LRDIMM isolation memory buffer data sheet," 2011.
- [26] Intel, "DDR3 LRDIMM system-level validation results on intel xeon e5-2600 v2 processor family," 2014.
- [27] —, "DDR3 RDIMM system-level validation results on intel xeon e5-2600 v2 processor family," 2014.
- [28] —, "Intel 64 and IA-32 architectures software developer's manual," 2014.
- [29] ITRS, "ITRS report 2012 update," 2012.
- [30] JEDEC, "JESD206: FBDIMM architecture and protocol," 2007.
- [31] —, "JESD79-3E: DDR3 SDRAM specification," 2010.
- [32] —, "JESD79-4: DDR4 SDRAM specification," 2012.
- [33] —, "JESD209-2F: LOW POWER DOUBLE DATA RATE 2 (LPDDR2)," 2013.
- [34] C. Kozyrakis, A. Kansal, S. Sankar, and K. Vaid, "Server engineering insights for large-scale online services," *IEEE micro*, vol. 30, no. 4, pp. 8–19, 2010.
- [35] B. C. Lee, E. Ipek, O. Mutlu, and D. Burger, "Architecting phase change memory as a scalable dram alternative," in *Proceedings of the 36th Annual International Symposium on Computer Architecture (ISCA)*, 2009.
- [36] K. Lim, J. Chang, T. Mudge, P. Ranganathan, S. K. Reinhardt, and T. F. Wenisch, "Disaggregated memory for expansion and sharing in blade servers," in *Proceedings of the 36th Annual International Symposium on Computer Architecture (ISCA)*, 2009.
- [37] K. Lim, D. Meisner, A. G. Saidi, P. Ranganathan, and T. F. Wenisch, "Thin servers with smart pipes: designing SoC accelerators for memcached," in *Proceedings of the 40th Annual International Symposium on Computer Architecture (ISCA)*, 2013.
- [38] K. Lim, Y. Turner, J. R. Santos, A. AuYoung, J. Chang, P. Ranganathan, and T. F. Wenisch, "System-level implications of disaggregated memory," in *2012 IEEE 18th International Symposium on High Performance Computer Architecture (HPCA)*, 2012.
- [39] Micron, "Rack up server performance with load-reduced DIMMs," <http://www.micron.com/products/dram-modules/lrdimm>.
- [40] —, "Tn-04-42: Memory module serial presence-detect introduction," 2002.
- [41] —, "Mobile LPDDR2-PCM 512mb, 1gb, x16, 1.8v/1.2v i/o 45nm phase change memory," 2012.
- [42] D. Molka, D. Hackenberg, R. Schone, and M. S. Muller, "Memory performance and cache coherency effects on an intel nehalem multiprocessor system," in *Proceedings of the 18th International Conference on Parallel Architectures and Compilation Techniques (PACT)*, 2009, pp. 261–270.
- [43] P. J. Nair, D.-H. Kim, and M. K. Qureshi, "Archshield: architectural framework for assisting DRAM scaling by tolerating high error rates," in *Proceedings of the 40th Annual International Symposium on Computer Architecture*, 2013.
- [44] J. Ousterhout, P. Agrawal, D. Erickson, C. Kozyrakis, J. Leverich, D. Mazières, S. Mitra, A. Narayanan, D. Ongaro, G. Parulkar *et al.*, "The case for RAMCloud," *Communications of the ACM*, vol. 54, no. 7, pp. 121–130, 2011.
- [45] C. Reiss, A. Tumanov, G. R. Ganger, R. H. Katz, and M. A. Kozuch, "Heterogeneity and dynamicity of clouds at scale: Google trace analysis," in *Proceedings of the Third ACM Symposium on Cloud Computing*, 2012.
- [46] P. Rosenfeld, E. Cooper-Balis, and B. Jacob, "Dramsim2: A cycle accurate memory system simulator," *Computer Architecture Letters*, vol. 10, no. 1, pp. 16–19, 2011.
- [47] D. Sanchez and C. Kozyrakis, "Zsim: fast and accurate microarchitectural simulation of thousand-core systems," in *Proceedings of the 40th Annual International Symposium on Computer Architecture (ISCA)*, 2013, pp. 475–486.
- [48] SGI, "White paper: Technical advances in the SGI UV architecture," 2012.
- [49] A. N. Udipi, N. Muralimanohar, R. Balasubramonian, A. Davis, and N. P. Jouppi, "Combining memory and a controller with photonics through 3d-stacking to enable scalable and energy-efficient systems," in *ACM SIGARCH Computer Architecture News*, 2011.